Paranal site-testing campaign of 2023: preliminary RINGSS results

Authors:*A. Tokovinin, E. Bustos*
Version: 3
Date: 2023-04-06
File: paranal/report1.tex

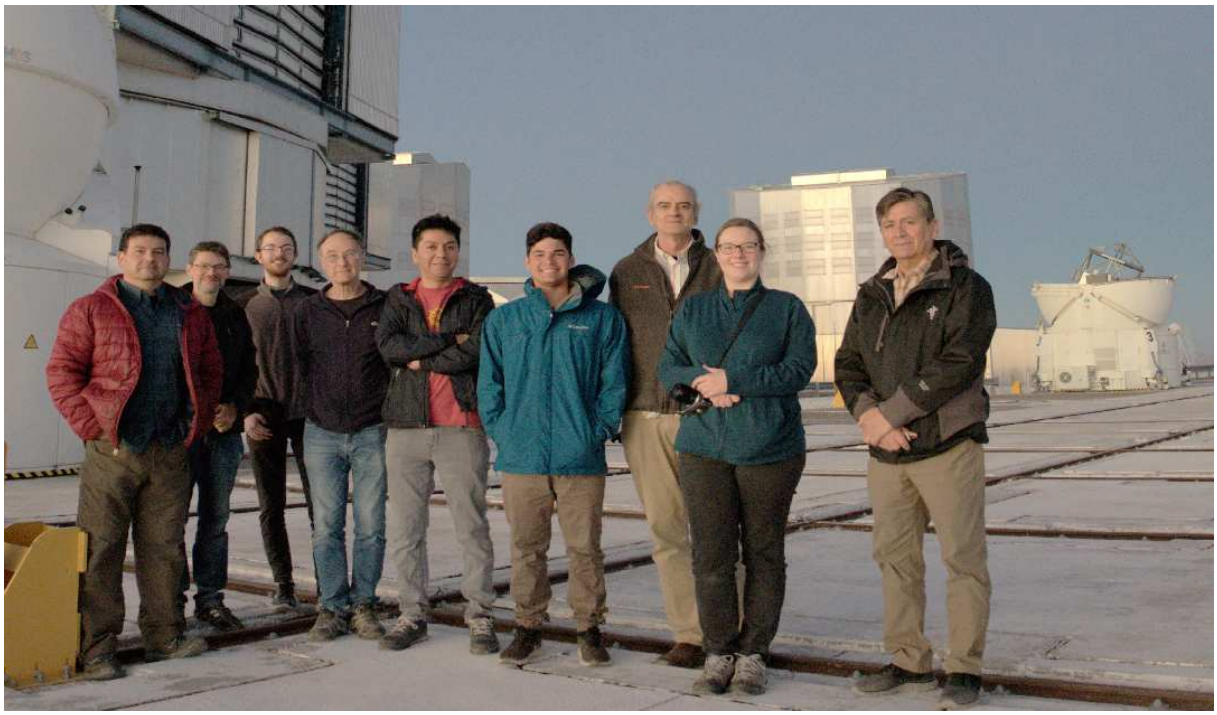

Figure 1: Participants of the 2023 Paranal profiling campaign on the VLT platform. Left to right: E. Bustos, M. Le Louarn, R. Griffiths, A. Tokovinin, B. Ayancan, A. Kamke, A. Guesalaga, L. Bardou, and A. Otarola. The open AT dome in the background houses the SCIDAR. Image credit: A. Otarola.

Figure 2: Portable turbulence profilers: RINGSS (left), SHIMM (center), and FASS (right, on the tripod).

1 Introduction: campaign and data

A campaign to characterize and compare various turbulence profilers has been organized by ESO (M. Le Louarn, A. Otarola). It took place from February 27 to March 4 2023, at Paranal. This note documents preliminary comparisons between RINGSS and other instruments, namely:

- RINGSS - our turbulence profiler, installed on a pier (aperture at 1.2 m above ground). The data are `.prof` files produced by the operational software with a 40-s cadence.
- DIMM and MASS on the VLT ASM seeing tower (6 m above ground, a few hundred meters away). The data are obtained from the ESO database via python scripts provided by A. Otarola.
- SCIDAR on the 1.8-m VLTI AT telescope, operated by J. Velasquez (ESO). The data were reduced by T. Butterly.
- SHIMM (Shack-Hartmann Image Motion Monitor) operated by the Durham team (R. Griffith and L. Bardou).
- FASS (Full-Aperture Scintillation sensor) operatede by the PUC team (A. Guesalaga, B. Ayancan, A. Kamke). FASS worked for three nights, March 1 to 3.

Note that the vistor instruments (RINGSS, SHIMM, FASS) were located close to each other on small pillars or tripods (Fig. 2), a few hundred meters away from the ASM tower and the SCIDAR. The viewing directions of the instruments did not always coincide.

2 RINGSS vs. ASM MASS-DIMM

The ASM data were accessed using python scripts provided by A. Otarola and slightly adapted. The output of the scripts is directed to the text files `seeing.txt` and `mass.txt`; the latter contains the integrated parameters (FA seeing and τ_0) and the profiles. The IDL codes `getsee.pro` and `getmass.pro` import the text into IDL structures and save them on the disk. All times are expressed as Julian days minus 2,400,000.

The RINGSS data are read from the `.stm` and `.prof` files into a single data structure `dat` using `readprof.pro`. The code `compare1.pro` matches the DIMM and MASS data to the moments of RINGSS observations (within 1 min) for comparion and generates the plots shown here. The total seeing in RINGSS is scintillation-based (the alternative parameter see2 based on the sectod motion is not used here).

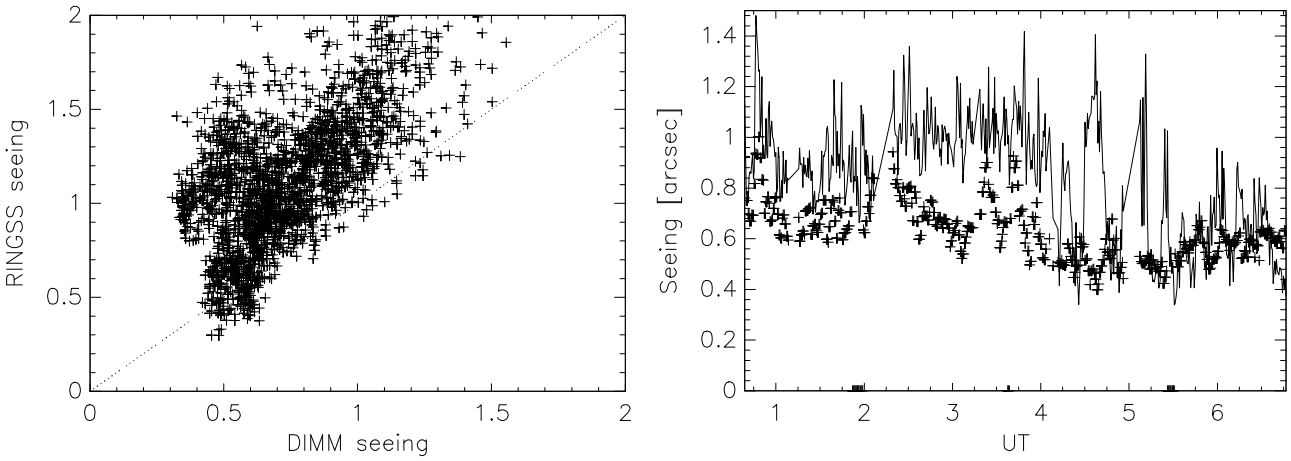

Figure 3: Left: comparison between the total seeing measured by RINGSS and DIMM on three nights. Right: temporal evolution of the seeing on Feb. 27/28 (line – RINGSS, crosses – ASM DIMM).

Comparison of the total seeing in Fig. 3 shows that most RINGSS and DIMM values are correlated with a slope larger than one, but there are points above the main group, where RINGSS measured a substantially larger seeing. The right panel illustrates the reason of this discrepancy, namely the extra ground-layer turbulence that affects RINGSS at some periods, but not always. The two instruments match well at times between those seeing spikes. On the last night, RINGSS measured an exceptionally good seeing of $0.33''$ for a short period without near-ground turbulence.

Figure 4 compares the free-atmosphere (FA) seeing from RINGSS (0.5 km layer and up) with the FA seeing measured by MASS. The right-hand panel compares the respective AO time constants τ_0. For RINGSS, it is computed using turbulence from 0.5 km up to match MASS (the ground layer is ignored).

Although both parameters measured by MASS correlate with RINGSS, some systematic deviations are apparent. Fig. 5, left, shows that the ratio of the FA seeing values and τ_0 are correlated. When MASS under-estimates the FA seeing, it over-estimates τ_0.

The right panel of Fig. 5 shows an interesting relation between total seeing and image motion. The rms motion of the ring center in each data cube (in pixels) is saved along with other data. It

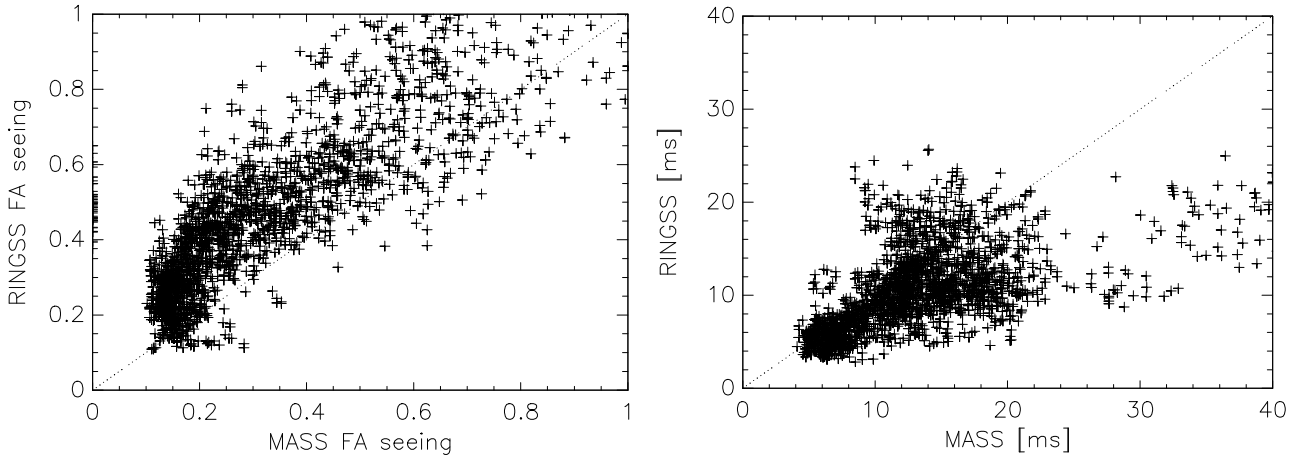

Figure 4: Comparison between RINGSS and MASS: free-atmosphere seeing (left) and atmospheric time constant (right). The dotted line is a 1:1 relation.

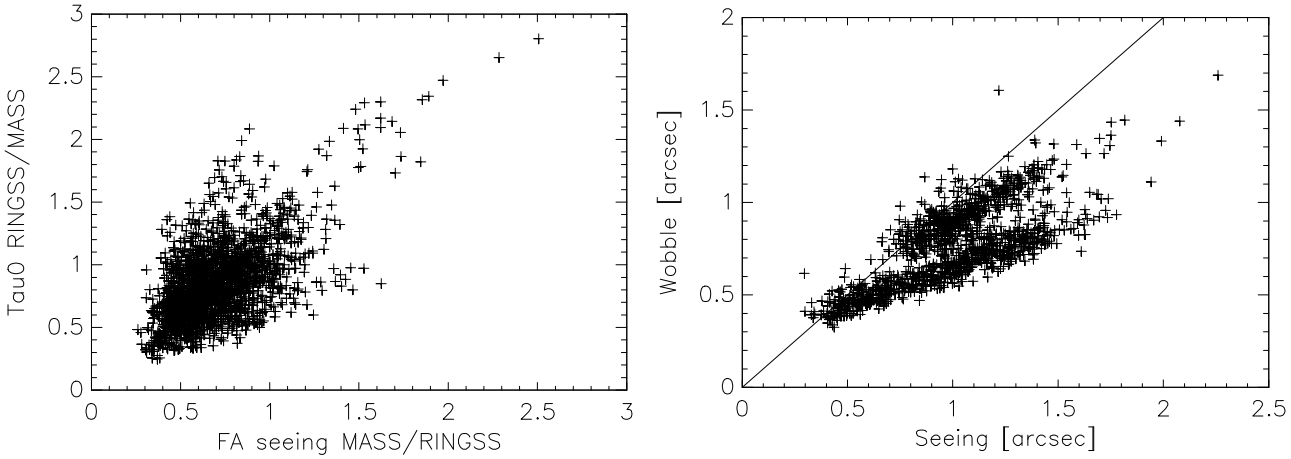

Figure 5: Left: ratio of the time constants vs. ratio of FA seeings for RINGSS and MASS. Right: correlation between total seeing in RINGSS and the image motion expressed as Gaussian FWHM.

is multiplied by the pixel size, $1.57''$, and the factor 2.35 to convert into FWHM of the equivalent Gaussian blur or "wobble". It turns out that this blur is equal to the seeing when it is good, meaning that the image motion is dominated by the wavefront tilts, while the telescope and mount shake are much smaller. The rms motions in X and Y are equal. The wind speed near the instrument was quite slow.

3 RINGSS vs. SCIDAR

The SCIDAR profiles were taken from the summary files provided by T. Butterly, one file per night. Each comma-separated line contains a date-time stamp, 5 numbers of unknown meaning (one of those

is seeing), and 400 numbers that define a 100-layer profile. For each layer, it lists the altitude (fixed, resolution 250 m), the $C_n^2 dh$ integral in $m^{1/3}$, the wind speed in m/s, and the wind direction. The wind is measured only for some layers with sufficient turbulent energy, zero otherwise. The $C_n^2 dh$ integrals equal -1 for layers above the upper distance limit. Each profile is based on a 2-min. data accumulation.

The SCIDAR data are read into an IDL structure using `readscidar.pro`. A total of 611 SCIDAR profiles covering 5 nights (with some gaps) are available. The code `compscidar.pro` matches the SCIDAR data to RINGSS (within 2 min) and produces the comparison plots. The SCIDAR profiles are multiplied by the notional RINGSS triangular functions to match the 8 RINGSS layers. The three lowest layers at 0, 0.25, and 0.5 km simply match the respective SCIDAR layers.

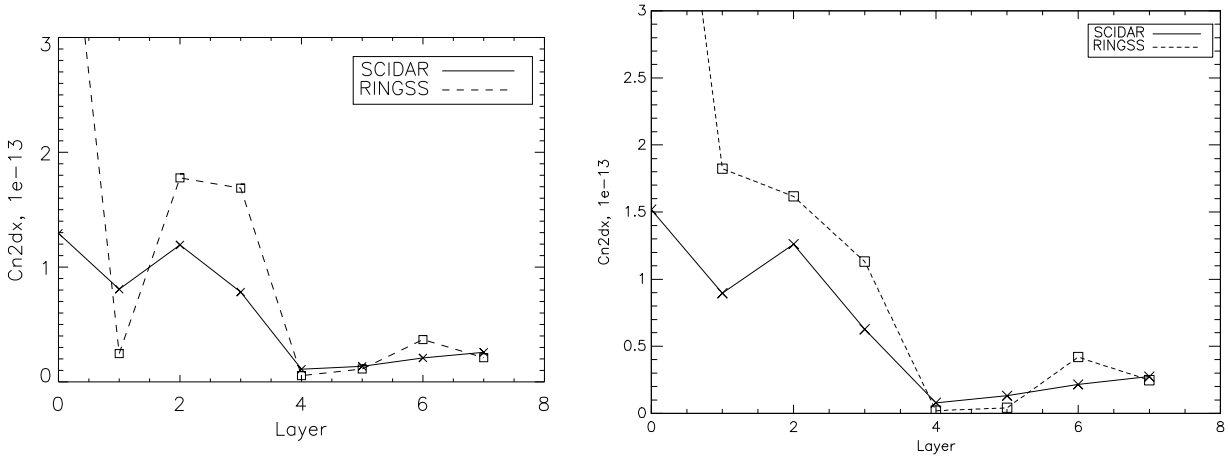

Figure 6: Mean profiles measured by RINGSS and SCIDAR on matched time. The SCIDAR profiles were smoothed to match the 8 RINGSS layers. The left plot is the standard RINGSS restoration (python) with 15 terms, the right-hand plot is produced using 17 terms with IDL.

The first comparison between RINGSS and SCIDAR revealed that RINGSS under-estimated turbulence in the 0.25-km layer, re-distributing it between the 0.5-km and ground layers. This is clear from the mean profiles shown in Fig. 6, left. However, when the maximum angular frequency term used for the profile-fitting is increased from m=15 to m=17, the turbulence is distributed more evenlly between these layers; higher layers are not affected (see the right panel). A delalied investigation of this difference[1] does not allow us to affirm that the standard $m = 15$ results are worse than $m = 17$. Re-distribution of the 0.25-km layer to adjacent layers has only a small effect on the data model, hence the 0.25-km results are less certain than for the other layers. Poor sensitivity to turbulence at low elevations is a common feature of all single-star profilers caused by the physival reasons, namely small amplitude of the scintillation and its fine spatial scale.

The comparison of FA seeing measured simultaneously by SCIDAR and RINGSS shows a reasonable correlation (Fig. 7, left). The FA seeing measured by MASS also agrees. If m=15 RINGSS profiles are used, the 0.5-km layer (which enters in the FA seeing calculation) is augmented by the lower tur-

[1] "Investigation of turbulence profile restoration in RINGSS," A. Tokovinin, 2023-03-28. http://www.ctio.noirlab.edu/~atokovin/ringss/profrestore.pdf

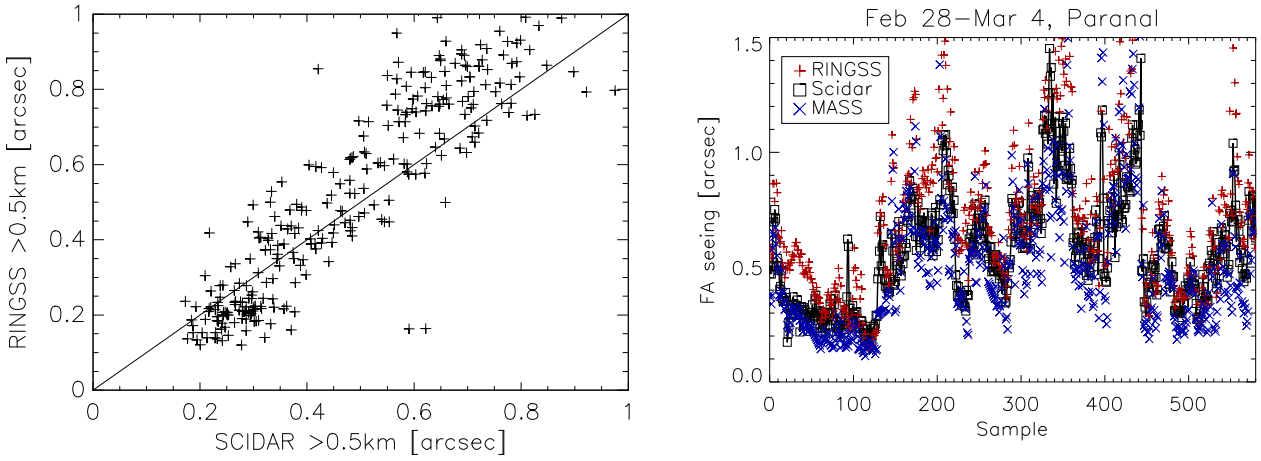

Figure 7: Comparison of FA seeing measured by SCIDAR and RINGSS (611 time-matched points). Left: X-Y plot, right: sequential plot, with the MASS FA seeing added.

buence and the FA seeing gets sometimes over-estimated. However, if the FA seeing is computed from 1km and and above, the agreement is good with m=15 as well.

Detailed comparison of profiles is given in Fig. 8. Note that a fraction of turbulence seen by SCIDAR at 16 km appears in the RINGSS 8-km layer. Turbulent spikes in the 0.5-km layer are seen by both instruments, but at different times.

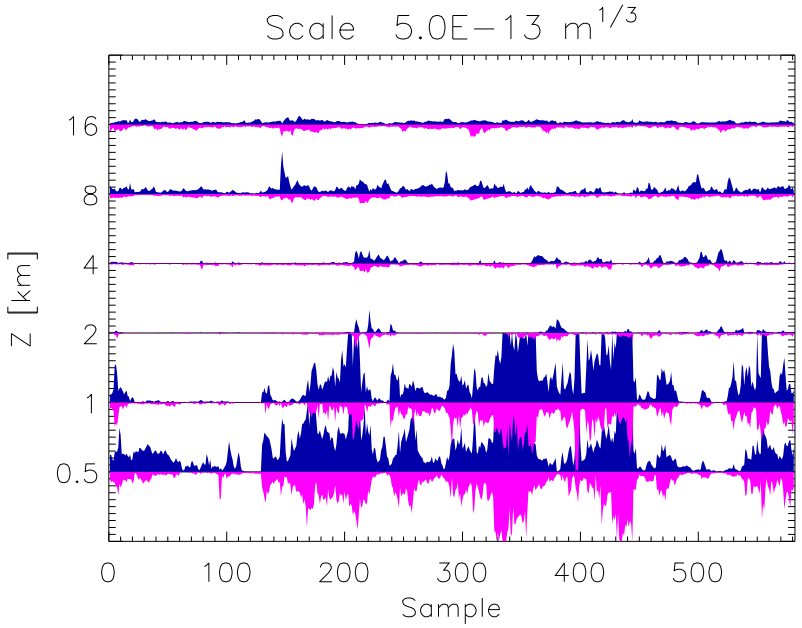

Figure 8: Turbulence profiles measured simultaneously by RINGSS (up-facing blue bars) and SCIDAR (down-facing magenta bars). SCIDAR is matched in resolution and time to RINGSS.

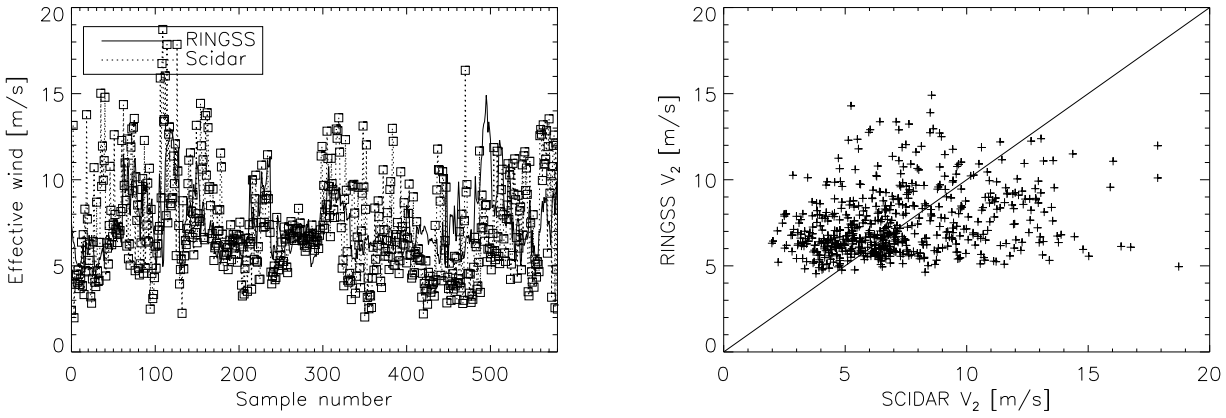

Figure 9: Effective wind speed measured by RINGSS and SCIDAR. Left: sequential plot, right: XY comparison.

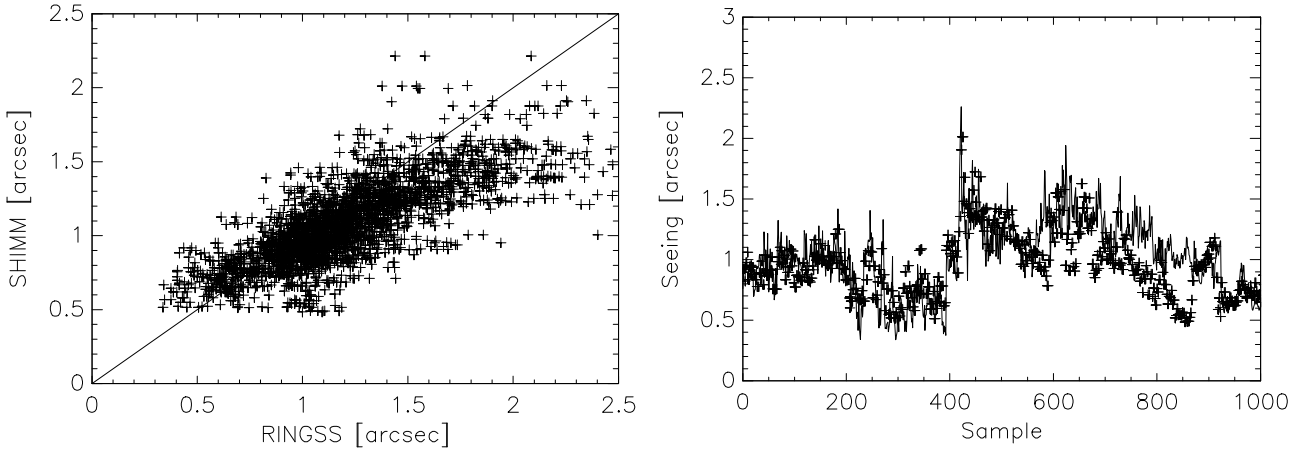

Figure 10: Comparison between the total seeing measured by RINNGSS and SHIMM. In the right panel, line is RINGSS, crosses – SHIMM.

Finally, Fig. 9 compares the effective wind speed V_2, used to estimate the AO time constant. It is measured by RINGSS using the Kornilov's method and computed for SCIDAR as a turbulence-weighted mean V^2, ignoring the two lowest layers below 0.5 km:

$$V_2^2 = \sum_{i'} V_{i'}^2 J_{i'} / \sum_i J_i \tag{1}$$

where i is the layer number, V_i is the wind speed, and J_i is the turbulence integral in this layer. The first sum includes only the layers i' where the wind speed is measured. The second sum in the denominator can include all layers i or only the layers with measured wind speed i'. These two alternative estimates of V_2 from SCIDAR differ substantially between themselves and with the RINGSS wind speed: the

first is smaller and the second is larger. However, the arithmetic mean of both estimates agrees quite well (this mean is used in Fig. 9).

4 RINGSS vs. SHIMM

The preliminary SHIMM data were provided by R. Griffiths in a python dataframe format. They were exported into a text file, ingested in IDL, and compared with the RINGSS seeing matched in time. We use the scintillation corrected r_0 values from SHIMM, which refer to 500 nm wavelength at zenith. The agreement is quite good (Fig. 10). The median RINGSS seeing is slightly larger than the SHIMM seeing, but this can be explained by the slight difference in the elevation (2 m vs 1.2 m) in presence of a strong ground-layer turbulence. One notes in the right panel of Fig. 10 how the two instruments match until the sample 500, when SHIMM begins to measure a systematically better seeing for a while.

5 RINGSS vs. FASS

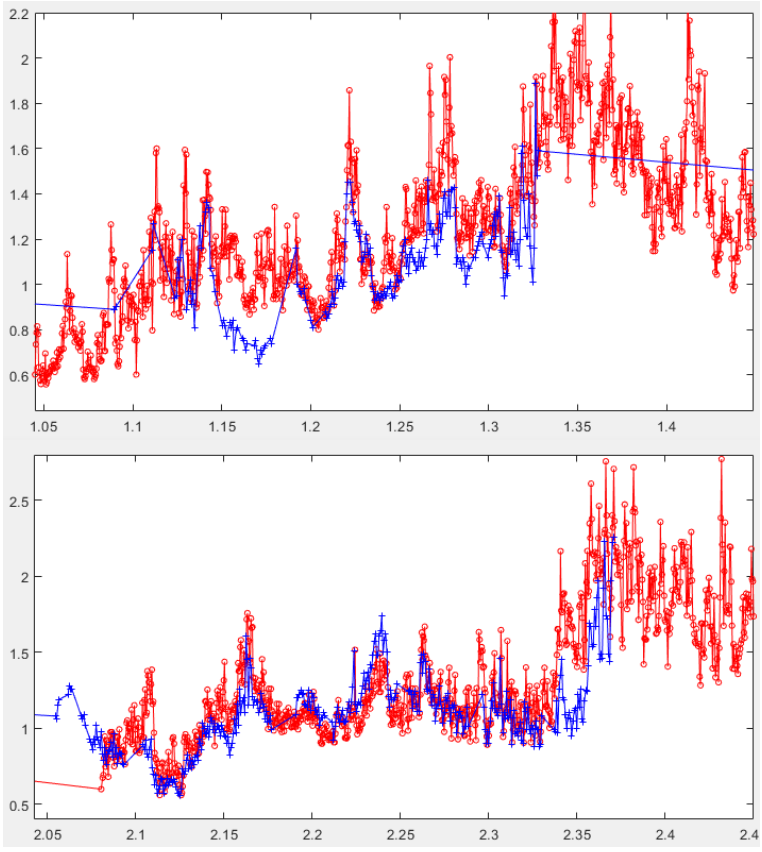

Figure 11: Comparison between the total seeing measured by RINGSS (red line) and FASS (blue line) on the nights of March 1 (top) and March 2 (bottom). This plot is provided by A. Guesalaga.

The full comparison between RINGSS and FASS is still pending. The plot in Fig. 11 was made by A. Guesalaga. It shows a good overall agreement. The FASS aperture was slightly higher than RINGSS and, as with SHIMM, this explains the diference at certain periods where the ground layer was strong.

6 Summary

Full results of the Paranal campaign will be published jointly by all its participants. This preliminary report is focused on the validation of RINGSS. Of particular interest is its comparison with the "reference" turbulence profiles, SCIDAR. A good agreement is found for the turbulence integral above 0.5 km (free-atmosphere seeing) and for the overall profiles, although RINGSS under-estimates the 0.25-km layer by assigning its turbulence to the neighboring layers. The full seeing measured by RINGSS shows a good agreement with two independent instruments working at the same location, SHIMM and FASS, and the expected partial agreement with the regular DIMM which operated from a 6-m tower. A much better agreement between RINGSS and DIMM is found at Cerro Tololo, where both instruments are installed at the same elevation.

We thank the organizers of the Paranal campaign, Angel Otarola and Miska Le Louarn, for inviting our team and providing material and logistic support. We are indebted to the SCIDAR operator Jose Velasquez and to Tim Butterly for timely data reduction.